DOI: 10.1002/chem.200701234

Isomeric Control of Protein Recognition with Amino Acid- and Dipeptide-Functionalized Gold Nanoparticles

Chang-Cheng You, Sarit S. Agasti, and Vincent M. Rotello*[a]

Abstract: Amino acid and dipeptide-functionalized gold nanoparticles (NPs) possessing L/D-leucine and/or L/D-phenylalanine residues have been constructed in order to target the surfaces of α-chymotrypsin (ChT) and cytochrome *c* (CytC). Isothermal titration calorimetry (ITC) was conducted to evaluate the binding thermodynamics and selectivity of these NP–protein interactions. The chirality of the NP end-groups substantially affects the resultant complex stability, with up to 20-fold differences seen between particles of identical hydrophobicity, demonstrating that structural information from the ligands can be used to control protein recognition.

Keywords: chirality · gold · molecular recognition · nanoparticles · proteins

Introduction

Protein-surface recognition features prominently in applications in broad fields of science and technology, such as control of cellular processes,[1,2] construction of biological sensors,[3] and creation of hybrid materials.[4] To date, various strategies to target protein–protein interactions have been proposed.[5] Macromolecules such as functionalized macrocyclic compounds,[6] polymers,[7] and dendrimers[8] have been used as artificial receptors in protein surface recognition, showing varying levels of ability to modulate the structures and functions of their protein targets.

Monolayer-protected nanoparticles (NPs) provide attractive scaffolds for the creation of protein surface receptors, since multiple functionalities could readily be introduced onto the convex NP surface to provide a versatile platform for biomacromolecule binding.[9] For example, multiple mannose-encapsulated gold NPs show affinities to concanavalin A 10–100 times higher than those of monovalent mannose ligands, due to the cooperativity of the adjacent ligands.[10] Our recent investigations have demonstrated that monolayer-protected NPs can bind to protein surfaces through simple charge-complementary interactions.[11] For instance, amino acid-functionalized gold NPs have shown tunable inhibition and stabilization/denaturation of α-chymotrypsin (ChT).[12,13] These preliminary results revealed that increasing the hydrophobicity of the NP ligands increases their binding affinity and the stability of the protein adsorbed on the NP surface,[12] a result substantiated in our recent calorimetric studies of nanoparticle–protein interactions.[14] In all cases there was little evidence for structural control of affinity, an important prerequisite for the specific recognition required for therapeutic applications.

Recent studies have shown that the surface chirality plays an important role in the interactions of proteins with solid surfaces.[15] In similar fashion, the use of enantiomeric and diastereotopic ligands on the surfaces of nanoparticles should provide a direct probe for examination of the role of side-chain structure on particle–protein interactions. To this end, we have fabricated a series of functionalized gold NPs featuring amino acid- and dipeptide-terminated monolayers displaying hydrophobic leucine and/or phenylalanine residues in their D and L forms.

ChT and cytochrome *c* (CytC) were chosen as target proteins. These two proteins feature positive surface charges (pI = 8.75 for ChT and pI 10.7 for CytC) but different surface characteristics. As shown in Figure 1, the ChT surface features hydrophobic "hot spots", while the CytC surface mainly consists of charged and uncharged hydrophilic residues. In this investigation we have explored the hydrophobic and chiral effects of the end-groups on complex formation. These studies demonstrate that subtle structural changes in the end-groups lead to substantial alterations in the particle affinity, with up to 20-fold differences observed between

[a] Dr. C.-C. You, S. S. Agasti, Prof. Dr. V. M. Rotello
Department of Chemistry, University of Massachusetts
710 North Pleasant Street, Amherst, MA 01002 (USA)
Fax: (+1) 413-545-4490
E-mail: rotello@chem.umass.edu

Supporting information for this article is available on the WWW under http://www.chemeurj.org/ or from the author.

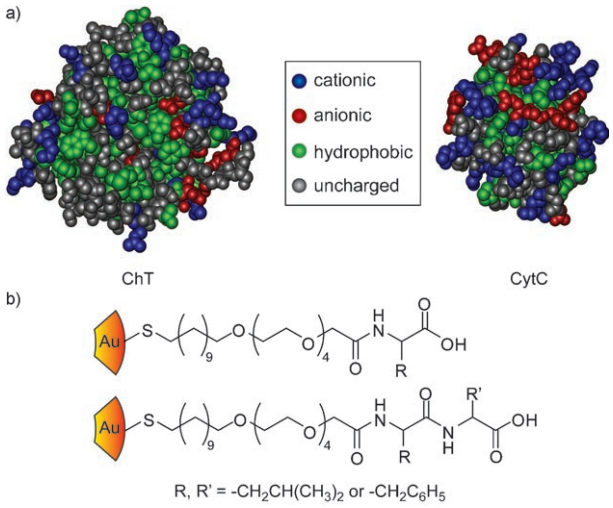

Figure 1. a) Surface structural features of ChT and CytC. b) Chemical structures of amino acid- and dipeptide-functionalized gold NPs.

particles with side-chains of identical hydrophobicity. These results demonstrate the feasibility of engineering nanoparticle–protein interfaces through use of the control provided through organic synthesis.

Results and Discussion

Synthesis of ligands and fabrication of nanoparticles: Dipeptide-functionalized gold NPs were prepared in a straightforward fashion as shown in Scheme 1. In these ligands, the alkyl chain (C_{11}) enhances the NP stability, and the tetra(ethylene glycol) (TEG) linker improves both the water solubility and the biocompatibility of the resultant NPs.[16] Dipeptides **2** were synthesized by coupling of *tert*-butoxycarbonyl-protected amino acids and amino acid methyl or ethyl esters in the presence of dicyclohexylcarbodiimide (DCC). Trityl-protected thiol ligands **3** were then obtained in good yields (≈70%) through the use of combinations of 1,1,1-triphenyl-14,17,20,23,26-pentaoxa-2-thiaoctacosan-28-oic acid (**1**) and dipeptides **2**, with activation by 1-ethyl-3-(3-dimethylaminopropyl)carbodiimide (EDC), *N*-hydroxybenzotriazole (HOBT), and diisopropylethylamine (DIPEA). Subsequently, treatment of compounds **3** with lithium hydroxide followed by trifluoroacetic acid (TFA) and triisopropylsilane (TIPS) led to the desired ligands (**4**) with both thiol anchor group and free carboxylic acid functionality. D-Amino acid-functionalized thiol ligands were also synthesized by a similar procedure (for synthetic details and characterization, see Supporting Information).

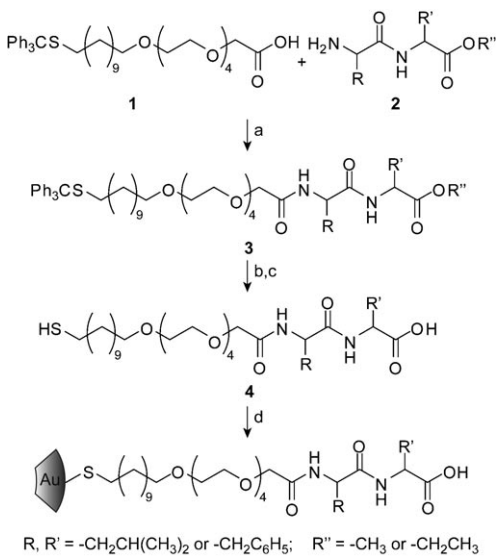

Scheme 1. Synthesis of dipeptide-functionalized thiol ligands and fabrication of the corresponding gold NPs: a) EDC, HOBT, DIPEA, CH_2Cl_2, RT, 36 h, 70%; b) LiOH, THF/H_2O, RT, 2 h, 100%; c) TFA, TIPS, CH_2Cl_2, RT, 12 h, 50–75%; d) C_5-AuNP, CH_2Cl_2, 2 d, quantitative.

Thiol ligands **4** were subjected to place-exchange reaction with pentane-1-thiol-coated gold NPs (C_5-AuNP, $d \approx 2$ nm)[17] in dichloromethane to afford the target NPs. Although ligands **4** and C_5-AuNP are highly soluble in CH_2Cl_2, the ligand-exchanged NPs precipitated from the solution, due to the presence of multiple carboxylate end-groups on the particle peripheries. Consequently, the target NPs could readily be collected by centrifugation followed by thorough rinsing with CH_2Cl_2. After drying under vacuum, the NPs were well dispersed in water. UV/Vis investigation revealed that their absorption features are consistent with their C_5-AuNP precursor and that no noteworthy surface plasma resonance band is present, indicating that no aggregation took place during the ligand exchange. The ^{1}H NMR spectra of the NPs display the proton signals of the corresponding ligands, but with significant broadening (see Supporting Information), typical for ligands anchored on NP surfaces. No proton signal for methyl groups is observed in C_5-AuNP, indicating that the place-exchange proceeded almost quantitatively.

Circular dichroism of nanoparticles: Circular dichroism (CD) spectra were recorded in order to evaluate the arrangement of amino acid and dipeptide functionalities on the NP surfaces. The aliphatic amino acid-/dipeptide-functionalized gold NPs show essentially no CD signal in the region from 600 to 190 nm. It has been demonstrated that the immediate attachment of chiral molecules onto metallic NPs can induce the corresponding CD responses in the particles.[18] In our case, however, the chiral centers of the amino acids are far away from the NP surface, and as a result do not affect the electron transitions of the gold cores. The CD results likewise indicate that no substantial interaction exists between the adjacent amino acid/dipeptide ligands, as a uniform arrangement of the amino acids organized through hydrogen bonding would be expected to generate CD signals in the far-UV region, as observed for micelles formed by amphiphilic amino acid ligands.[19]

The above conclusion is also supported by the CD spectra of aromatic amino acid-functionalized gold NPs: that is, phenylalanine-containing NPs. As shown in Figure 2, NP_

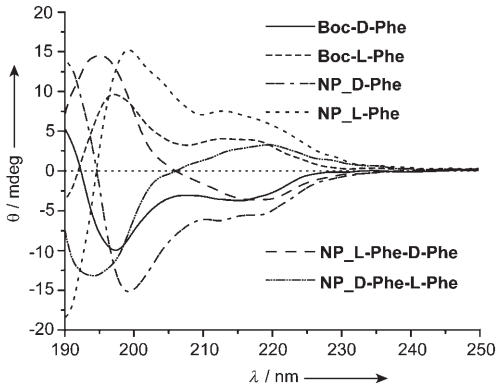

Figure 2. CD spectra of amino acid- and dipeptide-functionalized gold NPs containing D- or L-phenylalanine residues (0.5 μM) in sodium phosphate buffer (pH 7.4, 5 mM) at 25 °C (10 mm quartz cuvette). CD spectra of *tert*-butoxycarbonyl-protected D/L-phenylalanine (25 μM) are also depicted for comparison.

D-Phe and NP_L-Phe exhibit essentially the same CD spectra as their small molecular counterparts Boc-D-Phe and Boc-L-Phe, respectively, displaying a perfect mirror profile. As no new Cotton effect was observed, the amino acid functionalities on NP surfaces must have been behaving independently. From Figure 2 it can also be noted that the ellipticity (θ) of 0.5 μM NP_D-Phe (or NP_L-Phe) is about twice that of 25 μM Boc_D-Phe (or Boc_L-Phe). If the observed ellipticity is treated as the sum of the ellipticities of individual amino acids, it can be estimated that there are ca. 100 amino acid ligands on each NP, which agrees well with the previous conclusion that the ligand exchange is achieved quantitatively.[20] Dipeptide-functionalized NPs also exhibit mirror CD signals for the enantiomers, indicating that the same amounts of enantiometric ligands are loaded onto the respective NPs.

Isothermal titration calorimetry and binding stoichiometries: Isothermal titration calorimetry (ITC) can directly determine three thermodynamic quantities (i.e., ΔG, ΔH, and ΔS) through a single titration experiment. It has found extensive applications in evaluation of the energetics of biomolecular recognition.[21,22] Recently, ITC has been exploited to investigate the binding of amino acids and DNA bases to bare gold NPs[23] and in our preliminary studies of the interaction of amino acid-functionalized NPs with proteins.[14] In our current ITC experiments, aliquots of the protein solution were titrated into the sample cell containing NPs, and the heat change after each addition was recorded accordingly. A representative heat change profile for the complexation of ChT with NP_L-Phe-D-Phe is depicted in Figure 3a. It can be seen that a monotonic decrease in the exothermic heat of binding occurs with successive injections until saturation is reached. After subtraction of the heat of protein dilution, integration of the corresponding heat changes over time generated a typical sigmoidal titration curve as shown in Figure 3b. The ITC titration curve could be fitted into a model of a single set of identical binding sites by nonlinear

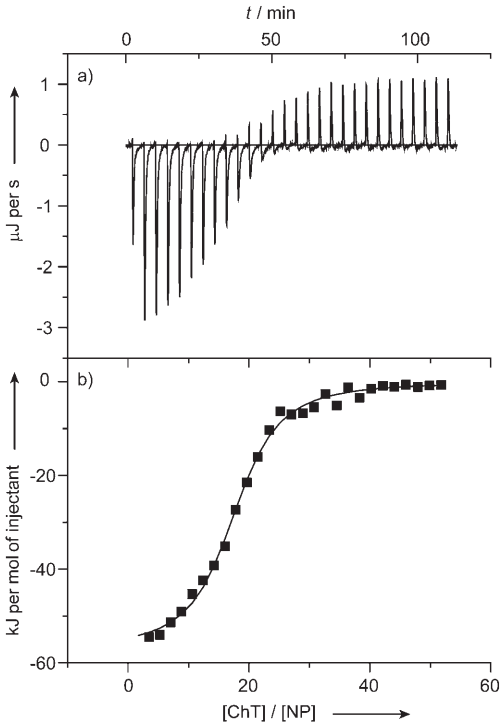

Figure 3. Isothermal titration calorimetry measuring the binding of ChT to NP_L-Phe-D-Phe: a) the heat change when ChT (400 μM) is titrated into NP_L-Phe-D-Phe (2.5 μM), and b) the integrated data (■) and the best fit to a nonlinear function with the assumption of a single type of binding sites (——).

least-squares regression, with the dissociation constants (K_D) and enthalpy changes (ΔH) simultaneously determined from the curve-fitting analysis. The Gibbs free energy changes (ΔG) and entropy changes (ΔS) were calculated from the experimentally determined K_D and ΔH values by use of classical thermodynamic equations (Table 1).

The titration of CytC solution into NPs generated heat output profiles drastically different from those obtained with ChT. When CytC is added to NP_L-Leu-L-Leu an endothermic process takes place, reaching a limiting value (Figure 4). An exothermic binding event is subsequently observed, approaching the second plateau. Models both of a single set and of two sets of binding sites were used in curve-fitting, but only the latter produces acceptable results. For the CytC-NP_L-Leu-L-Leu complexation, one binding event has a binding stoichiometry of 2.2, while the other binding event possesses a binding stoichiometry of 19.4. The thermodynamic quantities and the binding stoichiometries are compiled in Table 1.

In contrast with the single set of equivalent binding features for NP–ChT interactions, the complexation of CytC with the NPs studied featured two binding events: one is a stronger interaction with binding stoichiometries of 1.6–2.9, while the other is relatively weaker, with binding stoichiometries from 9.6 to 23.6. The origin of this bimodal binding is not currently known, but could arise either from the potential anisotropicity of the particle,[24] or through variation

Table 1. Dissociation constant (K_D), thermodynamic parameters (in kJ mol^{-1}), and binding stoichiometry (n) for the complexation of ChT and CytC with various nanoparticles in phosphate buffer (pH 7.4, 5 mM) at 30 °C.

Protein	Nanoparticle[b]	First binding event					Second binding event				
		K_D^1 [μM]	ΔG	ΔH	$T\Delta S$	n	K_D^2 [μM]	ΔG	ΔH	$T\Delta S$	n
ChT[a]	NP_Gly-Gly	2.14 ± 0.20	−32.9	−37.1 ± 1.9	−4.2	11.6	–				
	NP_L-Leu	2.45 ± 0.34	−32.6	−46.6 ± 2.5	−14.0	8.8	–				
	NP_D-Leu	1.38 ± 0.07	−34.0	−47.0 ± 0.3	−13.0	9.2	–				
	NP_L-Phe	2.29 ± 0.05	−32.7	−54.9 ± 2.8	−22.2	13.2	–				
	NP_D-Phe	1.12 ± 0.16	−34.5	−59.3 ± 0.9	−24.7	17.2	–				
	NP_L-Leu-L-Leu	1.32 ± 0.12	−34.1	−36.0 ± 0.6	−1.9	15.2	–				
	NP_L-Leu-D-Leu	1.05 ± 0.12	−34.7	−47.6 ± 1.6	−12.9	12.8	–				
	NP_L-Leu-L-Phe	0.81 ± 0.02	−35.3	−56.0 ± 1.0	−20.7	18.0	–				
	NP_L-Leu-D-Phe	0.58 ± 0.05	−36.2	−49.1 ± 0.5	−12.9	20.0	–				
	NP_L-Phe-D-Phe	0.82 ± 0.07	−35.3	−55.1 ± 1.6	−19.8	17.0	–				
	NP_D-Phe-L-Phe	1.17 ± 0.15	−34.5	−46.9 ± 3.6	−12.4	11.2	–				
	NP_D-Phe-D-Phe	0.44 ± 0.05	−36.9	−44.4 ± 1.3	−7.6	22.8	–				
CytC	NP_Gly-Gly	0.023 ± 0.004	−44.3	12.3 ± 2.0	56.6	1.8	1.78 ± 0.34	−33.4	4.9 ± 1.2	38.2	13.6
	NP_L-Leu	0.251 ± 0.012	−38.3	189.6 ± 3.0	227.9	2.0	1.95 ± 0.09	−33.1	2.3 ± 0.2	35.4	18.2
	NP_D-Leu	0.044 ± 0.008	−42.7	116.0 ± 0.1	158.5	1.6	1.12 ± 0.31	−34.5	6.6 ± 0.6	41.2	11.8
	NP_L-Phe	0.068 ± 0.006	−41.6	28.8 ± 0.1	70.4	2.2	1.51 ± 0.21	−33.8	13.1 ± 1.0	46.9	9.6
	NP_D-Phe	0.015 ± 0.005	−45.5	55.0 ± 4.5	100.6	2.6	3.02 ± 0.98	−32.0	13.8 ± 0.5	45.8	14.6
	NP_L-Leu-L-Leu	0.107 ± 0.015	−40.4	59.1 ± 1.6	99.5	2.2	1.29 ± 0.42	−34.2	25.5 ± 0.8	59.7	19.4
	NP_L-Leu-D-Leu	0.692 ± 0.034	−35.7	31.4 ± 1.6	67.2	1.8	1.74 ± 0.24	−33.4	21.7 ± 0.2	55.2	13.6
	NP_L-Leu-L-Phe	0.025 ± 0.003	−44.2	34.8 ± 0.7	78.9	2.9	1.62 ± 0.22	−33.6	24.6 ± 0.9	58.2	10.6
	NP_L-Leu-D-Phe	0.525 ± 0.097	−36.4	34.9 ± 0.7	71.4	2.0	1.48 ± 0.41	−33.8	21.2 ± 0.2	55.1	23.6
	NP_L-Phe-D-Phe	0.251 ± 0.077	−38.3	49.2 ± 3.2	87.6	2.2	0.98 ± 0.23	−34.9	25.7 ± 1.7	60.6	15.8
	NP_D-Phe-L-Phe	0.245 ± 0.114	−38.4	40.7 ± 4.7	79.1	1.8	1.00 ± 0.28	−34.8	21.2 ± 0.2	56.0	18.6
	NP_D-Phe-D-Phe	0.022 ± 0.004	−44.4	36.0 ± 2.6	80.3	2.6	0.79 ± 0.26	−35.4	21.7 ± 0.3	57.1	15.0

[a] The binding constants between ChT and NP_L-Leu or NP_L-Phe determined by ITC are smaller than the previously reported values, which were determined through enzyme activity assays (ref. [12]). The deviation most likely arises from the difference between these two systems. In enzyme activity assays, the solutions contained 8% *v/v* of ethanol/DMSO (90:10) in the 5 mM phosphate buffer used to dissolve the substrate. Moreover, *N*-succinyl-L-phenylalanine *p*-nitroanilide (SPNA, 2 mM), which may interfere in the NP–protein interactions, was added in the latter case to serve as the enzyme substrate. [b] The NP concentrations were determined on the basis of their average molecular weights by considering the size dispersion of the gold cores. The binding stoichiometries between ChT and NP_L-Leu and NP_L-Phe are somewhat different from the previously reported values, where the NP concentrations were obtained according to the UV absorbance of 2 nm gold cores.

of the CytC binding geometry due to the possible protein–protein interactions on the NP surface.[25]

The role of hydrophobicity in NP–protein complexation: In our previous studies on amino acid-functionalized nanoparticles, we observed a roughly linear correlation between the free energy (ΔG) of the ChT–nanoparticle binding and the hydrophobicity indices of the head-groups.[12] In the current case, varying degrees of correlation were observed between ΔG for the NP–protein interactions and the predicted octanol/water partition coefficients (log P) of the dipeptides.[26]

A rough correlation between the free energy changes of NP–ChT interactions and log P is observed, with the complex stability increasing substantially with increasing hydrophobicity of the amino acid/peptide head-groups (Figure 5a). In the case of CytC, however, there was little correlation between hydrophobicity and affinity. The Gibbs free energy changes for the first binding event between CytC and NPs range from −35.7 to −45.5 kJ mol^{-1} ($\Delta\Delta G_{max} = 9.8$ kJ mol^{-1}) with essentially no correlation with log P values. For the second binding event, the free energy changes vary less (from −32.0 to −35.4 kJ mol^{-1}), but there is once again little correlation between hydrophobicity and affinity.

The varying role of hydrophobicity in determining affinity can be explained by the difference in the surface features of ChT and CytC (Figure 1). ChT has 17 positively charged residues (14 Lys and 3 Arg) and some hydrophobic "hot spots" on the surface. The complexation between ChT and NPs is therefore driven by multivalent electrostatic interactions coupled with the assistance of hydrophobic interactions. CytC is a smaller protein that possesses more positively charged residues (i.e., 19 Lys and 2 Arg), with little surface hydrophobicity. The complexation between CytC and NPs is dominated by electrostatic interactions, with the contribution of hydrophobic interactions being less pronounced.

It is interesting to note that the complexation of ChT with all NPs is enthalpy-driven, with various levels of entropic loss observed. In contrast, the complex formation between CytC and NPs is dominated by the entropic contribution, which is attenuated by unfavorable enthalpy changes. Generally, it is believed that hydrophobic interactions are driven by entropy.[27,28] The complexation of ChT with NPs affords negative entropy changes, explicitly indicating that hydrophobic interaction acts as an accessory binding force. The thermodynamic contribution of this interaction is masked by other operations such as conformational restriction and solvation/desolvation. The former case leads to entropy loss, while desolvation is related to an entropy increase process. Therefore, the observed thermodynamic parameters merely reflect the overall outcomes of such compensatory effects.

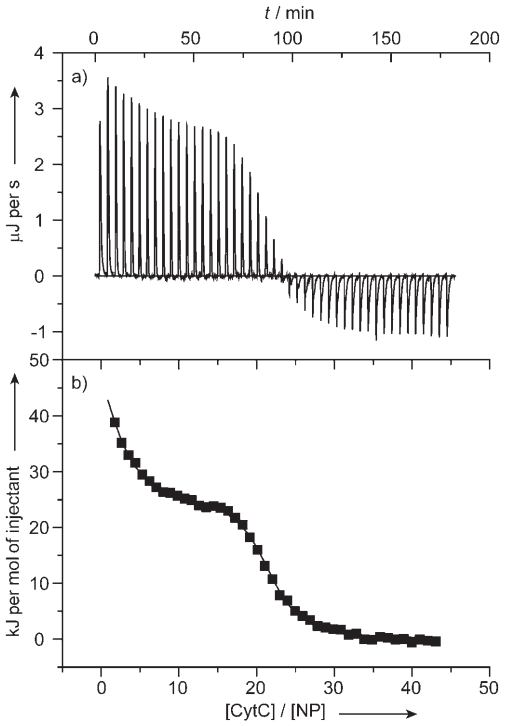

Figure 4. Isothermal titration calorimetry measuring the binding of CytC to NP_L-Leu-L-Leu: a) the heat change when CytC (1.0 mM) is titrated into NP_L-Leu-L-Leu (5 μM), and b) the integrated data (■) and the best fit to a nonlinear function with the assumption of two sets of binding sites (——).

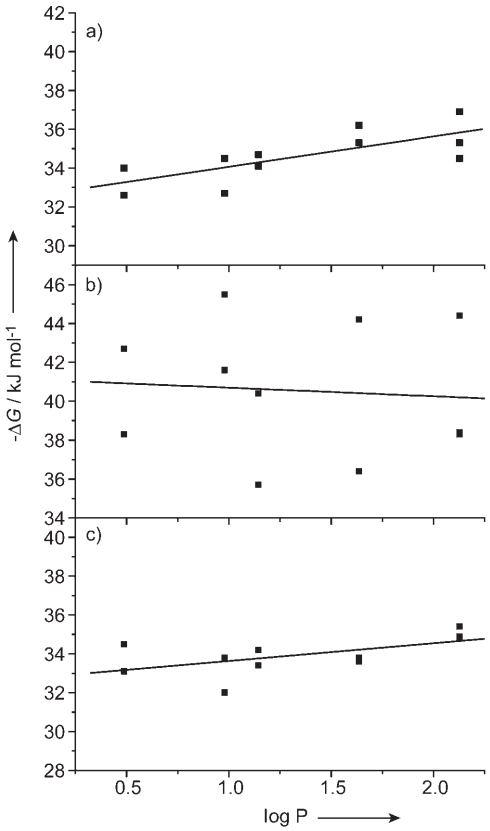

Figure 5. Correlation between Gibbs free energy changes (ΔG) for the NP–protein interactions and the logarithms of the octanol/water partition coefficient (log P) of NP functionalities. a) NP–ChT systems, b) first binding event for NP–CytC systems, and c) second binding event for NP–CytC systems.

Isomeric effects in the NP–protein interactions: Isomeric systems, in particular enantiomers and diastereomers, provide excellent tools for discerning specific and nonspecific interactions in complex systems.[29] From Table 1 and Figure 5, it can be seen that the NPs presenting enantiomeric or diastereoisomeric functionalities exhibit distinctly different binding affinities toward the proteins. For example, NPs bearing D-amino acids generally afford more stable complexes with ChT than their L isomer counterparts. The molecular selectivities of NP_D-Leu/NP_L-Leu and NP_D-Phe/NP_L-Phe are 1.8 and 2.0, respectively. An even higher value of 2.5 is observed for the NP_D-Phe-D-Phe and NP_D-Phe-L-Phe couple. The first binding event of NP–CytC interactions displays a stronger isomeric dependence on the NP functionalities. The highest selectivity of 21.4 is obtained for the NP_L-Leu-L-Phe/NP_L-Leu-D-Phe couple, while the second binding event of NP–CytC interactions affords a less pronounced isomeric effect, exhibiting the highest selectivity of 2.0 for NP_L-Phe/NP_D-Phe.

The drastically different isomeric effect on the first and the second binding events with CytC suggests that different binding modes might be involved in these processes. We have demonstrated that the NPs provide multivalent electrostatic interaction sites with the protein to form the supramolecular complexes, and that electrostatic forces govern the complex formation. In this context, the isomeric selectivity may arise from the matter of whether or not the complex formation is preferred with respect to the multiple electrostatic interactions. It is well documented that CytC can provide different binding domains upon complexation with its native and artificial partners.[25,30] It is thus reasonable to propose that CytC molecules adopt different orientations on different NP surfaces, in which the chiral amino acid side-chains play an important role in control over the orientation through steric repulsion and/or van der Waals attraction. In other words, the amino acid side-chain acts as a modulator to afford the isomeric selectivity.

It is interesting to compare the complex stabilities of enantiomers NP_L-Phe-D-Phe and NP_D-Phe-L-Phe with those of proteins, as the functionalities of these two NPs possess the same amino acid composition but inversed sequence. For the complexation with ChT, the former exhibits 1.4-fold higher binding affinity than the latter. This difference stems from the greater enthalpy gain during the complexation of NP_L-Phe-D-Phe. Upon binding to CytC, however, both NPs afford apparently identical binding affinities for either the first or the second binding events. In spite of the same Gibbs free energy changes, the enthalpy and entropy changes for these two NPs are completely different. That is, the complexation of CytC with NP_L-Phe-D-Phe exhibits a

more favorable entropy contribution, which is attenuated by unfavorable enthalpy gain.

Isomeric effects and enthalpy–entropy compensation: From the above discussion, it is clear that a compensatory relationship between enthalpy and entropy exists, a common phenomenon that has been found in various complexation processes.[27,31] Although the basis of such extrathermodynamic relationships is still under debate,[27] some efforts have been devoted to clarifying their physical significance.[32,33] In Figure 6a, the $T\Delta S$ values for the NP–protein

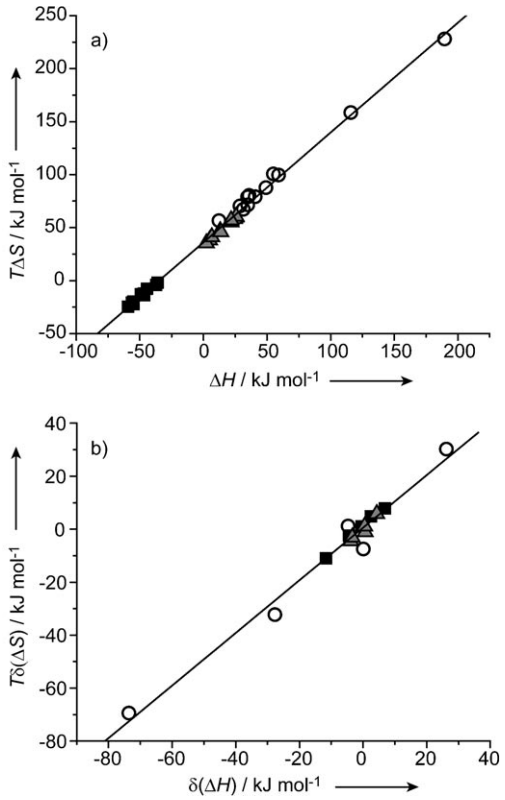

Figure 6. a) Compensation plot of entropy ($T\Delta S$) versus enthalpy (ΔH) for NP–protein interactions. b) Compensation plot for the differential entropy change ($T\delta(\Delta S)_{D/L}$) against the differential enthalpy change ($\delta(\Delta H)_{D/L}$) upon complexation of NPs bearing enantiomeric (diastereotopic) end-groups with proteins. ■: NP-ChT, ○: NP-CytC (**1**); ▲: NP-CytC (**2**).

interactions have been plotted against the ΔH values. An excellent linear correlation ($r=0.998$) was obtained, leading to a slope of 1.04 and an intercept of 36.1 kJ mol^{-1}, essentially identical to the values observed with amino acid-functionalized nanoparticles.[14] These coefficients can be taken as quantitative measurements of conformational changes and desolvation effects, respectively, during complex formation.[33] In our case, the near unit slope and the high value of the intercept in enthalpy–entropy compensation indicate that the system undergoes large conformational changes and extensive desolvation, which is significantly different from the "small" host–guest systems.[27,33] Thermodynamically, the unit slope also reflects that the contribution of the enthalpic gain by the system variation to the free energy change has been fully eliminated by the accompanying entropic loss.

Moreover, it can be noted that nanoparticles bearing enantiomeric end-groups display completely different enthalpy and entropy changes upon complexation with the same protein (i.e., $\Delta H_D \neq \Delta H_L$ and $T\Delta S_D \neq T\Delta S_L$) (Table 1). An important question arises: how do the thermodynamic quantities contribute to the isomeric selectivity over NP–protein interactions? The isomeric selectivity is defined as the differential Gibbs free energy changes for enantiomeric (or diastereoisomeric) NPs; a thermodynamic relationship can be readily established by using Equation (1):

$$\delta(\Delta G)_{D/L} = \Delta G_D - \Delta G_L = \delta(\Delta H)_{D/L} - T\delta(\Delta S)_{D/L} \quad (1)$$

The physical meaning of isomeric selectivity is the exchange efficiency of proteins from L isomer-functionalized NPs to their D isomer counterparts, which can be expressed as Equation (2):[34]

$$[NP_L \cdot protein] + NP_D \rightleftharpoons [NP_D \cdot protein] + NP_L \quad (2)$$

In this expression, structural features other than the chirality of the NP functionalities are cancelled, leaving only the contribution arising from structural (i.e., isomeric) differences. According to Equation (1), the isomeric selectivity lies in the compensation between $\delta(\Delta H)_{D/L}$ and $T\delta(\Delta S)_{D/L}$. In the case of a perfect compensation between these two parameters, the value of $\delta(\Delta G)_{D/L}$ would be equal to zero, resulting in no isomeric discrimination. Figure 6b shows the compensation plot for the enantiomeric exchange enthalpy ($\delta(\Delta H)_{D/L}$) and entropy ($T\delta(\Delta S)_{D/L}$). A linear correlation plot (Figure 6b) is obtained for these data points with a unit slope and a small value of intercept ($T\delta(\Delta S)_0 = 0.5$ kJ mol^{-1}).

In comparison with the common enthalpy–entropy plot (Figure 6a), an obviously more significant deviation from linearity is observed for the first binding event of NP–CytC interactions (Figure 6b), indicating that the large isomeric effect for this interaction arises from the unmatched enthalpy and entropy changes. In contrast, the smaller enthalpy–entropy compensation for NP–ChT and the second binding event of NP–CytC interactions lead to a reduced isomeric effect. As we have proposed, the spatial arrangement of CytC on the NP surface is different for the first and the second binding events. Therefore, the orientations of the proteins on the surface of NPs determine how the enantiomeric thermodynamics are shaped. On the other hand, the nanoparticles experience significant conformational changes, as revealed by enthalpy–entropy compensation analysis. Obviously, this process does not favor isomeric selectivity. In this regard, appropriate reduction of ligand freedom either by shortening the ligand length or by fastening the ligand position should provide better isomeric selectivity, as well as enhancement of the complex stability from the viewpoint of enthalpy–entropy compensation.

Conclusion

In summary, we have prepared a series of functional gold NPs bearing phenylalanine and/or leucine residues and have investigated their interactions with ChT and CytC. It has been demonstrated that the introduction of additional hydrophobic interaction sites can enhance the binding affinity to the protein that bears surface hydrophobic "hot spots" (ChT), with less pronounced effects on association with the highly charged protein (i.e., CytC). ITC investigation revealed that the NPs bearing enantiomeric and diastereoisomeric end-groups afford distinctly different binding affinities toward protein targets. This isomeric control of protein recognition comes from the noncompensatory enthalpy and entropy contributions. Clearly, the incorporation of chiral molecules onto monolayer-protected NPs through chemical approaches provides new opportunities for achieving specificity in the recognition of protein surfaces.

Experimental Section

Materials: α-Chymotrypsin (ChT, type I-S from bovine pancreas), cytochrome *c* (CytC, from horse heart), *tert*-butoxycarbonyl-amino acids, and amino acid methyl (or ethyl) esters were purchased from Sigma and used as received. All other chemicals were obtained from Aldrich or Fisher. Amino acid- and dipeptide-functionalized gold NPs were synthesized by the procedures depicted in Scheme 1, and detailed reaction conditions and characterization of the products can be found in the Supporting Information. Disodium hydrogen and sodium dihydrogen phosphate were dissolved in deionized, distilled water to make a phosphate buffer solution (5 mM) of pH 7.4, which was used as solvent in optical studies and isothermal titration calorimetry.

Circular dichroism: The circular dichroism (CD) spectra of NPs (0.5 μM) were measured on a JASCO J-720 spectropolarimeter with conventional quartz cuvettes (light path length = 10 mm) at 25 °C. The spectra were recorded as averages of three scans at a rate of 20 nm min^{-1}. The phosphate buffer background was subtracted from the raw spectra to give the final spectra.

Isothermal titration calorimetry: Microcalorimetric titrations were performed at 30 °C on a Microcal VP-ITC microcalorimeter. Each microcalorimetric titration experiment consisted of 30 or 45 successive injections of a constant volume (6 μL per injection) of ChT solution (400 μM) or CytC solution (1 mM) into a reaction cell (1.4 mL) charged with a NP solution (2.5 μM for ChT and 5.0 μM for CytC) in sodium phosphate buffer (5 mM, pH 7.4). The dilution heat of the protein solution upon addition to the buffer solution in the absence of NPs was determined in each run, with use of the same number of injections and concentration of ChT or CytC as in the titration experiments. The dilution enthalpies determined in these control experiments were subtracted from the enthalpies measured in the titration experiments. The ORIGIN program (version 7.0) supplied by Microcal Inc. was used to calculate the binding constants (K_D) and molar enthalpy changes (ΔH) of reaction from the titration curve by use of a model of a single set of identical sites (for ChT) or two sets of binding sites (for CytC). The molar Gibbs free energy changes (ΔG) and entropy changes (ΔS) of reaction were calculated from the experimentally determined K and ΔH values by use of the thermodynamic relationship of $\Delta G = RT\ln K_D = \Delta H - T\Delta S$. The reported thermodynamic quantities are averages of two parallel titration experiments.

Acknowledgement

This work was supported by the NIH (GM077173).

[1] G. Krauss, *Biochemistry of Signal Transduction Regulation*, 2nd ed., Wiley-VCH, Weinheim, **2001**.

[2] a) Y. S. Lee, P. Bergson, W. S. He, M. Mrksich, W. J. Tang, *Chem. Biol.* **2004**, *11*, 1139–1146; b) C. Boussard, T. Klimkait, N. Mahmood, M. Pritchard, I. H. Gilbert, *Bioorg. Med. Chem. Lett.* **2004**, *14*, 2673–2676; c) K. J. Capps, J. Humiston, R. Dominique, I. Hwang, D. L. Boger, *Bioorg. Med. Chem. Lett.* **2005**, *15*, 2840–2844; d) H. D. Arndt, *Angew. Chem.* **2006**, *118*, 4664–4673; *Angew. Chem. Int. Ed.* **2006**, *45*, 4552–4560; e) L. Romer, C. Klein, A. Dehner, H. Kessler, J. Buchner, *Angew. Chem.* **2006**, *118*, 6590–6611; *Angew. Chem. Int. Ed.* **2006**, *45*, 6440–6460.

[3] a) A. T. Wright, M. J. Griffin, Z. Zhong, S. C. McCleskey, E. V. Anslyn, J. T. McDevitt, *Angew. Chem.* **2005**, *117*, 6533–6536; *Angew. Chem. Int. Ed.* **2005**, *44*, 6375–6378; b) H. C. Zhou, L. Baldini, J. Hong, A. J. Wilson, A. D. Hamilton, *J. Am. Chem. Soc.* **2006**, *128*, 2421–2425; c) C.-C. You, O. R. Miranda, B. Gider, P. S. Ghosh, I.-B. Kim, B. Erdogan, S. A. Krovi, U. H. F. Bunz, V. M. Rotello, *Nat. Nanotechnol.* **2007**, *2*, 318–323.

[4] a) G. W. M. Vandermeulen, H.-A. Klok, *Macromol. Biosci.* **2004**, *4*, 383–398; b) T. Shiomi, T. Tsunoda, A. Kawai, H. Chiku, F. Mizukami, K. Sakaguchi, *Chem. Commun.* **2005**, 5325–5327; c) S. Srivastava, A. Verma, B. L. Frankamp, V. M. Rotello, *Adv. Mater.* **2005**, *17*, 617–621.

[5] a) P. L. Toogood, *J. Med. Chem.* **2002**, *45*, 1543–1558; b) L. Zhao, J. Chmielewski, *Curr. Opin. Struct. Biol.* **2005**, *15*, 31–34; c) H. Yin, A. D. Hamilton, *Angew. Chem.* **2005**, *117*, 4200–4235; *Angew. Chem. Int. Ed.* **2005**, *44*, 4130–4163.

[6] a) Y. Wei, G. L. McLendon, A. D. Hamilton, M. A. Case, C. B. Purring, Q. Lin, H. S. Park, C. S. Lee, T. Yu, *Chem. Commun.* **2001**, 1580–1581; b) R. K. Jain, A. D. Hamilton, *Angew. Chem.* **2002**, *114*, 663–665; *Angew. Chem. Int. Ed.* **2002**, *41*, 641–643; c) S. N. Gradl, J. P. Felix, E. Y. Isacoff, M. L. Garcia, D. Trauner, *J. Am. Chem. Soc.* **2003**, *125*, 12668–12669; d) S. Francese, A. Cozzolino, I. Caputo, C. Esposito, M. Martino, C. Gaeta, F. Troisi, P. Neri, *Tetrahedron Lett.* **2005**, *46*, 1611–1615.

[7] a) C. Renner, J. Piehler, T. Schrader, *J. Am. Chem. Soc.* **2006**, *128*, 620–628; b) B. S. Sandanaraj, R. Demont, S. V. Aathimanikandan, E. N. Savariar, S. Thayumanavan, *J. Am. Chem. Soc.* **2006**, *128*, 10686–10687; c) S. J. Koch, C. Renner, X. L. Xie, T. Schrader, *Angew. Chem.* **2006**, *118*, 6500–6503; *Angew. Chem. Int. Ed.* **2006**, *45*, 6352–6355.

[8] a) D. Paul, H. Miyake, S. Shinoda, H. Tsukube, *Chem. Eur. J.* **2006**, *12*, 1328–1338; b) M. L. Wolfenden, M. J. Cloninger, *Bioconjugate Chem.* **2006**, *17*, 958–966; c) A. Klaikherd, B. S. Sandanaraj, D. R. Vutukuri, S. Thayumanavan, *J. Am. Chem. Soc.* **2006**, *128*, 9231–9237.

[9] a) C. M. Niemeyer, *Angew. Chem.* **2003**, *115*, 5944–5948; *Angew. Chem. Int. Ed.* **2003**, *42*, 5796–5800; b) E. Katz, I. Willner, *Angew. Chem.* **2004**, *116*, 6166–6235; *Angew. Chem. Int. Ed.* **2004**, *43*, 6042–6108; c) T. Pellegrino, S. Kudera, T. Liedl, A. M. Javier, L. Manna, W. J. Parak, *Small* **2005**, *1*, 48–63; d) N. L. Rosi, C. A. Mirkin, *Chem. Rev.* **2005**, *105*, 1547–1562; e) C.-C. You, M. De, V. M. Rotello, *Curr. Opin. Chem. Biol.* **2005**, *9*, 639–646; f) C.-C. You, A. Verma, V. M. Rotello, *Soft Matter* **2006**, *2*, 190–204; g) R. Baron, B. Willner, I. Willner, *Chem. Commun.* **2007**, 323–332.

[10] C.-C. Lin, Y.-C. Yeh, C.-Y. Yang, G.-F. Chen, Y.-C. Chen, Y.-C. Wu, C.-C. Chen, *Chem. Commun.* **2003**, 2920–2921.

[11] a) N. O. Fischer, C. M. McIntosh, J. M. Simard, V. M. Rotello, *Proc. Natl. Acad. Sci. USA* **2002**, *99*, 5018–5023; b) R. Hong, N. O. Fischer, A. Verma, C. M. Goodman, T. Emrick, V. M. Rotello, *J. Am. Chem. Soc.* **2004**, *126*, 739–743.

[12] a) C.-C. You, M. De, G. Han, V. M. Rotello, *J. Am. Chem. Soc.* **2005**, *127*, 12873–12881; b) C.-C. You, M. De, V. M. Rotello, *Org. Lett.* **2005**, *7*, 5685–5688.

[13] C.-C. You, S. S. Agasti, M. De, M. J. Knapp, V. M. Rotello, *J. Am. Chem. Soc.* **2006**, *128*, 14612–14618.
[14] M. De, C.-C. You, S. Srivastava, V. M. Rotello, *J. Am. Chem. Soc.* **2007**, *129*, 10747–10753.
[15] a) M. Geva, F. Frolow, M. Eisenstein, L. Addadi, *J. Am. Chem. Soc.* **2003**, *125*, 696–704; b) J. J. Gray, *Curr. Opin. Struct. Biol.* **2004**, *14*, 110–115.
[16] a) A. G. Kanaras, F. S. Kamounah, K. Schaumburg, C. J. Kiely, M. Brust, *Chem. Commun.* **2002**, 2294–2295; b) J. C. Love, L. A. Estroff, J. K. Kriebel, R. G. Nuzzo, G. M. Whitesides, *Chem. Rev.* **2005**, *105*, 1103–1169.
[17] M. Brust, M. Walker, D. Bethell, D. J. Schiffrin, R. Whyman, *J. Chem. Soc. Chem. Commun.* **1994**, 801–802.
[18] a) T. Li, H. G. Park, H.-S. Lee, S.-H. Choi, *Nanotechnology* **2004**, *15*, S660–S663; b) H. Yao, K. Miki, N. Nishida, A. Sasaki, K. Kimura, *J. Am. Chem. Soc.* **2005**, *127*, 15536–15543; c) C. Gautier, T. Bürgi, *J. Am. Chem. Soc.* **2006**, *128*, 11079–11087; d) M.-R. Goldsmith, C. B. George, G. Zuber, R. Naaman, D. H. Waldeck, P. Wipf, D. N. Beratan, *Phys. Chem. Chem. Phys.* **2006**, *8*, 63–67.
[19] a) M. Shinitzky, R. Haimovitz, *J. Am. Chem. Soc.* **1993**, *115*, 12545–12549; b) S. Roy, D. Das, A. Dasgupta, R. N. Mitra, P. K. Das, *Langmuir* **2005**, *21*, 10398–10404; c) D. Khatua, J. Dey, *J. Phys. Chem. B* **2007**, *111*, 124–130.
[20] There are ca. 100 thiol ligands for 2 nm gold nanoparticles, see: M. J. Hostetler, J. E. Wingate, C.-J. Zhong, J. E. Harris, R. W. Vachet, M. R. Clark, J. D. Londono, S. J. Green, J. J. Stokes, G. D. Wignall, G. L. Glish, M. D. Porter, N. D. Evans, R. W. Murray, *Langmuir* **1998**, *14*, 17-30.
[21] a) M. L. Doyle, *Curr. Opin. Biotechnol.* **1997**, *8*, 31–35; b) I. Jelesarov, H. R. Bosshard, *J. Mol. Recognit.* **1999**, *12*, 3–18.
[22] a) R. J. Bingham, J. B. Findlay, S. Y. Hsieh, A. P. Kalverda, A. Kjellberg, C. Perazzolo, S. E. Philips, K. Seshadri, C. H. Trinh, W. B. Turnbull, G. Bodenhausen, S. W. Homans, *J. Am. Chem. Soc.* **2004**, *126*, 1675–1681; b) S. L. Kazmirski, M. Podobnik, T. F. Weitze, M. O'Donnell, J. Kuriyan, *Proc. Natl. Acad. Sci. USA* **2004**, *101*, 16750–16755; c) P. Buczek, M. P. Horvath, *J. Mol. Biol.* **2006**, *359*, 1217–1234; d) B. K. Muralidhara, S. S. Negi, J. R. Halpert, *J. Am. Chem. Soc.* **2007**, *129*, 2015–2024.
[23] a) H. Joshi, P. S. Shirude, V. Bansal, K. N. Ganesh, M. Sastry, *J. Phys. Chem. B* **2004**, *108*, 11535–11540; b) A. Gourishankar, S. Shukla, K. N. Ganesh, M. Sastry, *J. Am. Chem. Soc.* **2004**, *126*, 13186–13187.
[24] a) A. M. Jackson, J. W. Myerson, F. Stellacci, *Nat. Mater.* **2004**, *3*, 330–336; b) A. M. Jackson, Y. Hu, P. J. Silva, F. Stellacci, *J. Am. Chem. Soc.* **2006**, *128*, 11135–11149; c) G. A. DeVries, M. Brunnbauer, Y. Hu, A. M. Jackson, B. Long, B. T. Neltner, O. Uzun, B. H. Wunsch, F. Stellacci, *Science* **2007**, *315*, 358–361.
[25] a) H. R. Brosshard, *Cytochrome c: A Multidisciplinary Approach*, University Science Books, Sausalito, CA, **1996**, pp. 373–396; b) I. Bertini, G. Cavallaro, A. Rosato, *Chem. Rev.* **2006**, *106*, 90–115; c) H. Pelletier, J. Kraut, *Science* **1992**, *258*, 1748–1755; d) J. E. Erman, G. C. Kresheck, L. B. Vitello, M. A. Miller, *Biochemistry* **1997**, *36*, 4054–4060; e) K. F. Wang, Y. J. Zhen, R. Sadoski, S. Grinnell, L. Geren, S. Ferquson-Miller, B. Durham, F. Millett, *J. Biol. Chem.* **1999**, *274*, 38042–38050; f) P. L. Edmiston, J. E. Lee, S.-S. Cheng, S. S. Saavedra, *J. Am. Chem. Soc.* **1997**, *119*, 560–570; g) J. Zhou, J. Zheng, S.-Y. Jiang, *J. Phys. Chem. B* **2004**, *108*, 17418–17424; h) J.-S. Xu, E. F. Bowden, *J. Am. Chem. Soc.* **2006**, *128*, 6813–6822; i) I. D. G. Macdonald, W. E. Smith, *Langmuir* **1996**, *12*, 706-713.
[26] The octanol/water partition coefficients (log P) were calculated on the basis of acyl amino acids or dipeptides by use of QSAR implemented in Hyperchem 7.0. The values for Ac-Leu, Ac-Phe, Ac-Leu-Leu, Ac-Leu-Phe, and Ac-Phe-Phe are 0.488, 0.979, 1.145, 1.635, and 2.126, respectively.
[27] K. N. Houk, A. G. Leach, S. P. Kim, X. Zhang, *Angew. Chem.* **2003**, *115*, 5020–5046; *Angew. Chem. Int. Ed.* **2003**, *42*, 4872–4897.
[28] J. N. Israelachvili, *Intermolecular Surface Forces*, 2nd ed., Academic Press, London, **1992**.
[29] a) T. D. Booth, D. Wahnon, I. W. Wainer, *Chirality* **1997**, *9*, 96–98; b) A. Berthod, *Anal. Chem.* **2006**, *78*, 2093–2099.
[30] H. Bayraktar, C.-C. You, V. M. Rotello, M. J. Knapp, *J. Am. Chem. Soc.* **2007**, *129*, 2732–2733.
[31] a) L. Liu, Q.-X. Guo, *Chem. Rev.* **2001**, *101*, 673–695; b) D. J. Winzor, C. M. Jackson, *J. Mol. Recognit.* **2006**, *19*, 389–407.
[32] a) J. D. Dunitz, *Chem. Biol.* **1995**, *2*, 709–712; b) D. H. Williams, E. Stephens, D. P. O'Brien, M. Zhou, *Angew. Chem.* **2004**, *116*, 6760–6782; *Angew. Chem. Int. Ed.* **2004**, *43*, 6596–6616.
[33] a) Y. Inoue, T. Hakushi, *J. Chem. Soc. Perkin Trans. 2* **1985**, 935–946; b) Y. Inoue, Y. Liu, L.-H. Tong, B.-J. Shen, D.-S. Jin, *J. Am. Chem. Soc.* **1993**, *115*, 10637–10644; c) Y. Inoue, T. Wada, *Adv. Supramol. Chem.* **1997**, *4*, 55–96; d) M. V. Rekharsky, Y. Inoue, *Chem. Rev.* **1998**, *98*, 1875–1917.
[34] Rekharsky and Inoue have discussed the chiral recognition of cyclodextrins in terms of either host or guest exchange, which minimize the contribution of the nominal thermodynamic items, see: a) M. V. Rekharsky, Y. Inoue, *J. Am. Chem. Soc.* **2000**, *122*, 4418–4435; b) M. V. Rekharsky, Y. Inoue, *J. Am. Chem. Soc.* **2002**, *124*, 813–826.

Received: August 7, 2007
Published online: October 30, 2007

